Hindawi
Journal of Food Biochemistry
Volume 2023, Article ID 5521661, 14 pages
https://doi.org/10.1155/2023/5521661

Research Article

Antibacterial, Antibiofilm, Antiswarming, and Antioxidant Activities of Flavonoids Isolated from *Allium colchicifolium* Leaves

Mohammad Bagher Majnooni,[1,2] **Syed Mustafa Ghanadian**,[3] **Mahdi Mojarrab**,[2] **Gholamreza Bahrami**,[2,4] **Kamran Mansouri**,[4] **Arezoo Mirzaei**,[5] **and Mohammad Hossain Farzaei**[2]

[1]*Student Research Committee, Kermanshah University of Medical Sciences, Kermanshah, Iran*
[2]*Pharmaceutical Sciences Research Center, Health Institute, Kermanshah University of Medical Sciences, Kermanshah, Iran*
[3]*Department of Pharmacognosy, School of Pharmacy and Pharmaceutical Sciences, Pharmaceutical Sciences Research Center, Isfahan University of Medical Sciences, Isfahan, Iran*
[4]*Medical Biology Research Center, Health Technology Institute, Kermanshah University of Medical Sciences, Kermanshah, Iran*
[5]*Department of Bacteriology and Virology, Faculty of Medicine, Isfahan University of Medical Science, Isfahan, Iran*

Correspondence should be addressed to Syed Mustafa Ghanadian; ghannadian@gmail.com and Mohammad Hossain Farzaei; mh.farzaei@gmail.com

Received 22 February 2023; Revised 5 May 2023; Accepted 1 July 2023; Published 18 August 2023

Academic Editor: Charalampos Proestos

Allium (A.) species are one of the most widespread plants in the world, which have played a special role in terms of nutrition, treatment, and economy since long ago. This study is the first report on the phytochemical and biological activities of *A. colchicifolium*. Five flavonoids, including isorhamnetin (compound **1**), quercetin (compound **2**), morin (compound **3**), isorhamnetin-3-O-glucoside (compound **4**), and quercetin 3-O-glucoside (compound **5**), were isolated and purified for the first time from *A. colchicifolium* leaves. All isolated flavonoids showed antibacterial and antibiofilm activities. Compound **3** revealed prominent antibacterial activities against *Staphylococcus* (*S.*) *aureus* and *Proteus* (*P.*) *mirabilis*. Also, compounds **3** and **5** showed the highest antibiofilm activities on *S. aureus* and *P. mirabilis*, respectively. The docking study results showed that compounds **3**, **4**, and **5** had the most robust interactions with two critical proteins in biofilm formation, including staphylococcal accessory regulator A (SarA) and mannose-resistant *Proteus*-like fimbriae H (MrpH). Besides, compounds **2** and **3** revealed significant antioxidant activities in 2, 2-diphenyl-1-picrylhydrazyl (DPPH) and ferric (Fe^{3+})-reducing antioxidant power (FRAP) tests compared to the other compounds and positive controls. Also, the ADMET (absorption, distribution, metabolism, excretion, and toxicity) prediction assay showed that compounds **1**, **2**, and **3** have suitable physicochemical and pharmacokinetic properties. The results of this study confirm that the flavonoids isolated from the leaves of *A. colchicifolium* can be promising candidates for use in the pharmaceutical and food industries.

1. Introduction

The genus *Allium* (*A.*) of the family Liliaceae, with 800 to 900 species, is one of the largest monocotyledonous plants. The *Allium* species have fantastic nutritional, therapeutic, and economic value. Onion (*A. cepa*), garlic (*A. sativum*), shallot (*A. ascalonicum*/*A. hirtifolium*), leek (*A. ampeloprasum*), Welsh onion (*A. fistulosum*), bear's garlic (*A. ursinum*), and chives (*A. schoenoprasum*) are among the most important edible species of this genus, which since ancient times (2800–3200 B.C) until now as medicine and part of the people's diet [1–3]. Steroidal saponins, organosulfur compounds, and fructooligosaccharides are the major compounds that are isolated from flowers, leaves, and bulbs of

Allium species [4, 5]. Besides, the plants of the *Allium* genus are known as one of the rich natural sources of polyphenolic compounds, especially flavonoids such as quercetin, isorhamnetin, kaempferol, apigenin, myricetin, luteolin, and their glycosylated derivatives [6–9]. Kaempferol-3-O-(6″-feruloyl)-sophoroside and quercetin-3-O-(6-trans-feruloyl)-β-D-glucopyranosyl-(1 ⟶ 2)-β-D-glucopyranoside-7-O-β-D-glucopyranoside from *A. tuberosum* shoots [10, 11], kuwanon K, xanthomicrol, and rhamnazin from *A. cepa* bulbs [12], and kaempferol-3-O-neohesperidoside-7-O-glucuronide from *A. microdictyon* [13] are among the flavonoids that have recently been isolated from the *Allium* species. Also, several biological and pharmacological activities, including anticancer, antihypercholesterolemia, cardioprotective, neuroprotective, anti-inflammation, and antidiabetic, have been reported for *Allium* flavonoids [14–16]. Also, the *Allium* flavonoids showed prominent antioxidant and antimicrobial activities in several investigations [3, 17]. Besides, *Allium* spp and its flavonoids showed antibacterial activities via inhibiting the bacterial defence mechanisms, including quorum sensing, biofilm formation, and swarming [18, 19]. Quecan and coworkers reported that quercetin and its glucoside derivatives, including quercetin 4-O-glucoside and quercetin 3,4-O-diglucoside, found in *Allium cepa* revealed the antiquorum sensing, antibiofilm, and antiswarming effects on *Pseudomonas aeruginosa* and *Serratia marcescens*. This study showed that quercetin 4-O-glucoside and quercetin 3,4-O-diglucoside had a high affinity with CviR and LasR as two main quorum sensing proteins [20]. Taxifolin and apigenin [21], kaempferol and naringenin [22], myricetin [23], and luteolin [24] are other *Allium* flavonoids that showed antiquorum-sensing activities. On the other hand, *Allium* flavonoids revealed high antioxidant potential. Kim and coworkers isolated four antioxidant flavonoids, including kaempferol-3-O-β-D-glucopyranoside, quercetin 3-O-β-D-glucopyranoside, isorhamnetin 3-O-β-D-glucopyranoside, and quercetin 3-O-β-D-xylopyranoside from *Allium sativum* shoots and leaves [25]. Also, three flavonoids, including chrysoeriol, chrysoeriol-7-O(2″-O-E-feruloyl)-β-D-glucoside, and isorhamnetin-3-β-D-glucoside isolated from *Allium vineale* showed antioxidant properties [26]. Another study showed that kaempferol glycoside derivatives, luteolin, and apigenin identified in *Allium roseum* flowers and leaves have prominent antibacterial and antioxidant activities [27]. On the other hand, *A. colchicifolium* is one of the native species of *Allium* in western Iran, especially in Kermanshah province, which is commonly known as Koul in Kurdish. *A. colchicifolium* (synonym = *A. haussknechtii* and *A. straussii*) leaves are used raw as a garnish and salad and cooked as local food. It is also used as an antirheumatoid, antilipidemic, and anti-infective in folk medicine [28–30]. To the best of our knowledge, there are no reports of phytochemical studies and biological/pharmacological effects of *A. colchicifolium*. Therefore, due to the critical roles of *Allium* flavonoids mentioned above, the flavonoids of *A. colchicifolium* leaves were isolated and identified using chromatographic and spectroscopic techniques in the present study using one- and two-dimensional nuclear magnetic resonance (NMR) and mass spectrometry (MS). Also, these flavonoids' antibacterial and antioxidant activities were evaluated, and an *in-silico* study investigated the antibiofilm mechanisms of these compounds.

2. Materials and Methods

2.1. General Experimental Procedures. The NMR spectra were conducted on a Bruker Avance AV 400 ^{1}H-NMR (400 MHz, DMSO-d6) and ^{13}C-NMR (100 MHz, DMSO-d6). The ^{13}C-NMR multiplicities of resonances were specified by the DEPT spectrum. Heteronuclear multiple-bond correlation spectroscopy ^{1}H-^{13}C connections were identified with the HMBC spectrum. Mass analysis was done by the Agilent 1200 series liquid chromatography (LC) system (Agilent Technologies, Germany) coupled with an Agilent 6410 triple quadrupole MS and electrospray ionization (ESI) with a capillary voltage of 4,000 V (Agilent Technologies, Palo Alto, CA, USA). Thin layer chromatography (TLC) was conducted on the Merck TLC silica gel (SiO_2, Germany) with chloroform/methanol ($CHCl_3$: MeOH, 9 : 1) and discerned by spraying 1% natural product reagent (2-aminoethyl diphenylborinate, Merck, Germany) and 1% ceric sulfate (Merck, Germany) solution in 10% sulfuric acid (Mojalali, Iran), followed by heating using hair dryer for about 2-3 minutes. Column chromatography (CC) was performed on polyamide SC6 (Roth, Germany) and Sephadex-LH (Pharmacia fine chemicals, Uppsala, Sweden). $CHCl_3$ and MeOH (Merck, Germany) were used as elution solvents in developing columns.

2.2. Plant Material. The whole plant of *A. colchicifolium* was bought on April 2021 from local vegetable markets in Kermanshah province, Iran. The plant was identified by Prof. Seyed Mohammad Masoumi (Department of Biology, Faculty of Science, Razi University, Kermanshah, Iran) and confirmed by comparison to the voucher specimen (No. 160-036-001-001) already deposited in the Department of Pharmacognosy, Faculty of Pharmacy, Kermanshah University of Medical Sciences. Also, its morphological characteristics, including the arrangement of inflorescences, the colour of flowers, and the shape of its leaves and bulbs, were consistent with the information provided by Fritsch and Abbasi [28, 31].

2.3. Extraction and Isolation. The air-dried leave powders (7 kg) of the *A. colchicifolium* were extracted at room temperature with hexane, $CHCl_3$, $CHCl_3$/MeOH (9 : 1), and MeOH (each 20 L for 3 days), consecutively. To extract the flavonoid content, the $CHCl_3$/MeOH extract (100 g) as a semipolar part was suspended in bicarbonate solution (1%, 1 L) and extracted by diethyl ether (1 L, two times) in a separation funnel to remove the lipophilic content. The pH of the aqueous solution was adjusted to 3.0 by adding HCl (0.2 N) and re-extracted using ethyl acetate (1 L, three times) [32, 33]. The ethyl acetate extract rich in phenolics was concentrated and submitted on polyamide SC6 column chromatography using a stepwise gradient solvent system of

$CHCl_3$: MeOH (98 : 2, Fr.1; 96 : 4, Fr.2; 94 : 6, Fr.3; 92 : 8, Fr.4; 90 : 10, Fr.5; 88 : 12, Fr.6; 86 : 14, Fr.7; 84 : 16, Fr.8; 82 : 18, Fr.9; 80 : 20, Fr.10; each 500 mL). According to the TLC profile (SiO_2, CHCl3: MeOH, 9 : 1) visualized by natural product reagent (2-aminoethyl Diphenylborinate 1%), Fr.6 and Fr.7 with yellow spots were selected as fractions rich in flavonoids. Fr.6 was submitted on a Sephadex LH-20 column (3 × 80 cm; Methanol) in 10 mL collection size tubes from Fr.6.1 to Fr.6.4. Fr.6.2 was obtained in a pure state as compound **4** (58 mg). Fr.6 – 1, Fr.6 – 3, and Fr.6 – 4 were recrystallized in cold methanol to take compounds **1** (21 mg), **2** (25 mg), and **3** (15 mg). Fr.7 was submitted on the same column and yielded compound **5** (32 mg).

2.4. Antibacterial, Antibiofilm, and Antiswarming Activities

2.4.1. Microbial Strains and Culture Maintenance. *Staphylococcus aureus* (ATCC 25923) and *Proteus mirabilis* (ATCC 7002) as a member of gram-positive and gram-negative bacteria were chosen and provided by the Microbiology Department of Medical Sciences University of Isfahan, Iran. Strains were cultured on blood, eosin-methylene blue (EMB), and MacConkey agar and enriched in trypticase soy broth (TSB) and trypticase soy agar (TSA) agar (Himedia, India) plates at 37°C.

2.4.2. Antibacterial Activities. The antibacterial activity of the crude extract and isolated flavonoids was assayed by the minimum inhibitory concentration (MIC) values using the broth microdilution method with 96-well microtiter plates according to Mirzaei et al. [34]. Two-fold serial dilutions of the samples (500, 250, 125, 62.5, 31.25, 15.62, 7.81, 3.9, and 1.9 μg/ml) were prepared in 1 ml TSB. The inoculum of the strains was prepared in TSB-containing glucose (1% w/v) (Himedia, India), and the turbidity was adjusted to 0.5 McFarland and 1/1000 diluted to obtain final turbidity, approximately 0.5×10^5colony-forming units (CFU)/ml. 75 μl of the solution of the compounds and 75 μl of the bacterial inoculum were inserted into the wells of a microtiter plate and incubated at 37°C for 24 h. The results of MIC were visually assayed, and the minimum concentration of bacteria growth was reported as MIC [34]. To find the exact dilution for MIC_{50}, an ELISA microplate reader evaluated the bacterial growth at 595 nm. The results were reported as MIC_{50}, which is equivalent to the minimum concentration that inhibits 50% of the bacterial growth [35].

$$\%\ \text{antibacterial activities} = 1 - \frac{(\text{OD negative control} - \text{OD tested compounds})}{(\text{OD negative control})} \times 100. \quad (1)$$

2.4.3. Antibiofilm Activities. The antibiofilm activities of the crude extract and isolated flavonoids were investigated by the modified crystal violet assay. Twofold serial dilutions of the compounds in the LB broth were prepared from 500 μg/ml to 1.96 μg/ml in sterile 96-well microtiter plates. A 10 μl of overnight incubation strains suspension (0.5 McFarland) was added to each well containing 100 μl LB broth and different concentrations of crude extracts and the flavonoid compounds. Then, they were incubated at 37°C for 48 h. The positive control included LB media with bacteria, and the negative control included LB media without bacteria and compounds. After incubation, the wells were rinsed with 200 μl of phosphate-buffered saline to remove the loosely attached bacteria. After that, the wells were fixed with 200 μl of 96% ethanol for 15 minutes. The wells were dried for 30 min at 37°C, and biofilms formed by adherent cells in the wells were stained with 1% (w/v) crystal violet for 10 min. Then excess crystal violet was gently washed five times with deionized water. Optical densities (OD_{595}) of the stained adherent bacteria were determined after adding 200 μl acetone-ethanol (33%–80%) with the proportion of 1 : 1 using an ELISA microplate reader, and absorbance was recorded. The antibiofilm activity ratio of the compounds was calculated with the following formula and reported as $MIBC_{50}$ equivalent to the minimum concentration inhibiting 50% of bacterial biofilm formation [35]. The positive control was the untreated bacteria. The test was done in triplicate.

$$\%\ \text{antibiofilm activities} = 1 - \frac{(\text{OD positive control} - \text{OD tested compounds})}{(\text{OD positive control})} \times 100. \quad (2)$$

2.4.4. Antiswarming Activities. For antiswarming effects, various concentrations of the crude extract and isolated flavonoids ((500, 250, 125, 62.5, 31.25, 15.62, 7.81, 3.9, and 1.9 μg/ml) were mixed with 10 ml of the LB agar medium containing overnight cultures of *P. mirabilis*. After incubating the plates at 37°C for 3 days, the inhibition of swarming activities was recorded by measuring the area of the colonies in mm [34, 36].

2.5. Antioxidant Activities

2.5.1. DPPH Assay. The antioxidant activity of the samples was measured by the ability of bleaching of the purple-coloured methanol solution of DPPH [37]. The different concentrations of the crude extract and test compounds were prepared by serial dilution in methanol. Then, 1 ml of DPPH (0.5 mM in methanol) was added with 2 ml of 0.1 M sodium acetate buffer (pH 5.5). The mixtures were vigorously shaken and kept at room temperature in a dark place for 30 min. The absorbance was measured at 517 nm against the blank (containing all reagents except the test compound). The ascorbic acid was used as a positive control. The percentage of scavenging (% scavenging) of DPPH radical was calculated using the following equation:

$$\%\ \text{scavenging} = \frac{(\text{A0} - \text{As})}{\text{A0}} \times 100. \quad (3)$$

In this formula, A0 is the absorbance of the blank and as is the absorbance of the test compounds. The IC50 value represents the concentration of the test compounds causing 50% scavenging.

2.5.2. Reducing Power. The FRAP assay was performed based on the total antioxidant capacity assay kit (Naxifer™, Navandsalamat, Iran). In brief, 250 μL working solution (acetate buffer (pH 3.6), 2,4,6-tripyridyl-s-triazine (TPTZ, 40 mM) solution, and $FeCl_3{\cdot}6H_2O$ solution (20 mM) (5 : 1:1, v/v/v)) was added to 5 μL of compounds (**1–5**) and the crude extract and kept at 37°C for 5 minutes. Then, the absorbance was measured at 593 nm using a microplate reader. The standard calibration curve of the $FeSO_4$ was obtained at different concentrations (0, 0.2, 0.4, 0.6, 0.8, and 1 μM), and the total antioxidant capacity of the compounds was calculated as $FeSO_4\mu$M equivalent. All determinations were done in triplicate and compared with butylated hydroxyanisole as a positive control [38].

2.6. Molecular Docking. The X-ray crystal structures of the two target proteins staphylococcal accessory regulator A (SarA) (PDB ID: 2FNP) and mannose-resistant *Proteus*-like fimbriae H (MrpH) (PDB ID: 6Y4E) were downloaded from the Protein Data Bank (PDB; https://www.RCSB.org) [39]. The cocrystalized ligand, cofactor, and water molecules were removed. Polar hydrogens were added by AutoDock tools version 1.5.6, and energy minimization was performed using the Molegro Virtual Docker [40]. To prepare the structures of the ligands generated by ChemScketch, adding hydrogens and energy minimization were done using Chimera software [41]. To identify the binding site of SarA, the Computed Atlas of Surface Topography of proteins (CASTp) server (https://sts.bioe.uic.edu/castp/) was utilized. The residues of the predicted binding site include Phe110, Leu113, Ser114, Thr117, Tyr118, Lys121, Glu223, and Leu224 in chain A and Thr141, Tyr142, Glu145, Asn146, His159, and Leu160 in chain B. The binding site of MrpH was determined based on its cocrystallographic ligand (Arg118, Thr116, Ile140, His74, Asn82, His72, His117, and Gly81) [42]. Docking was conducted using AutoDock Vina in PyRx 0.8. Grid boxes were set with dimensions (Angestrom) of $X = 28.2522$, $Y = 24.6015$, and $Z = 25.7223$ and coordinates of $X = -5.8249$, $Y = -8.0013$, and $Z = -1.8428$ and with dimensions of $X = 23.2163$, $Y = 22.5185$, and$Z = 20.4395$ and coordinates of $X = 4.7575$, $Y = 8.4108$, and $Z = -6.4855$ for SarA and MrpH, respectively. After docking calculations, LigPlot+ was used to analyze protein-ligand interactions [43].

2.7. In Silico ADMET Studies. ADMET (absorption, distribution, metabolism, excretion, and toxicity) properties are dominant factors that should be evaluated in the early stages of drug discovery [44]. In this study, the physiochemical properties, including the molecular weight, the number of H-bond receptors and H-bond donors, TPSA (topological polar surface area), and lipophilicity (MLOGP) and pharmacokinetic parameters including gastrointestinal (GI) absorption, blood-brain barrier (BBB) permeability, P-glycoprotein (P-gp) substrate, and CYP450 2C9 (CYP2C9) inhibitor of isolated flavonoids (compound **1–5**) were predicted by SwissADME web tool (https://www.swissadme.ch). Also, drug likeness was investigated according to Lipinski's rule of 5 (Ro5). Drug likeness assesses the chances for a molecule to become an oral drug with respect to bioavailability [45, 46]. Besides, toxicity, carcinogenicity, and cardiotoxicity endpoint such as human ether-a-go-go-related gene (HERG) inhibition of compounds (**1–5**) were predicted using the admetSAR database (https://lmmd.ecust.edu.cn/admetsar1/) [47].

3. Results and Discussion

3.1. Identification of the Isolated Pure Compounds. Edible plants, including *Allium* spp, have long been the focus of researchers to discover new medicinal molecules due to their high safety. They could be used in the food industry as safe and low-risk preservatives, one of the richest natural sources of polyphenols, especially flavonoids [48–50]. Therefore, in this study, the extraction, purification, and phytochemical investigation of flavonoids in *A. colchicifolium*, widely used for nutritional and therapeutic purposes, have been addressed. In the present study, the $CHCl_3$/MeOH extract (9 : 1) with a yield of 12% was selected for phytochemical analysis, which resulted in the isolation and identification of five flavonoids (Figure 1).

Compound **1** was obtained as a pale-yellow solid with a positive reaction to flavonoid natural product reagent (2-aminoethyl diphenylborinate 1%). The ^{1}H-NMR spectra showed five protons in the aromatic region, two *meta*-coupled doublets at δ_H 6.31 (1H, d, $J = 2.02$ Hz) and 6.60 (1H, d, $J = 2.02$ Hz) corresponding to H-6 and H-8, two *ortho*-coupled proton signals at δ_H 7.06 (1H, d, $J = 8.41$ Hz) and 7.80 (1H, dd, $J = 8.41$, 2.06 Hz) related to H- 5′ and H-6′, and a doublet at δ_H 7.87 (1H, d, $J = 2.06$ Hz) related to H-2′ proton, as well as a methoxy resonance at δ_H 3.95 (3H, s), with HMBC correlation with C-3′ (δ_C 135.77). It also showed signals of four

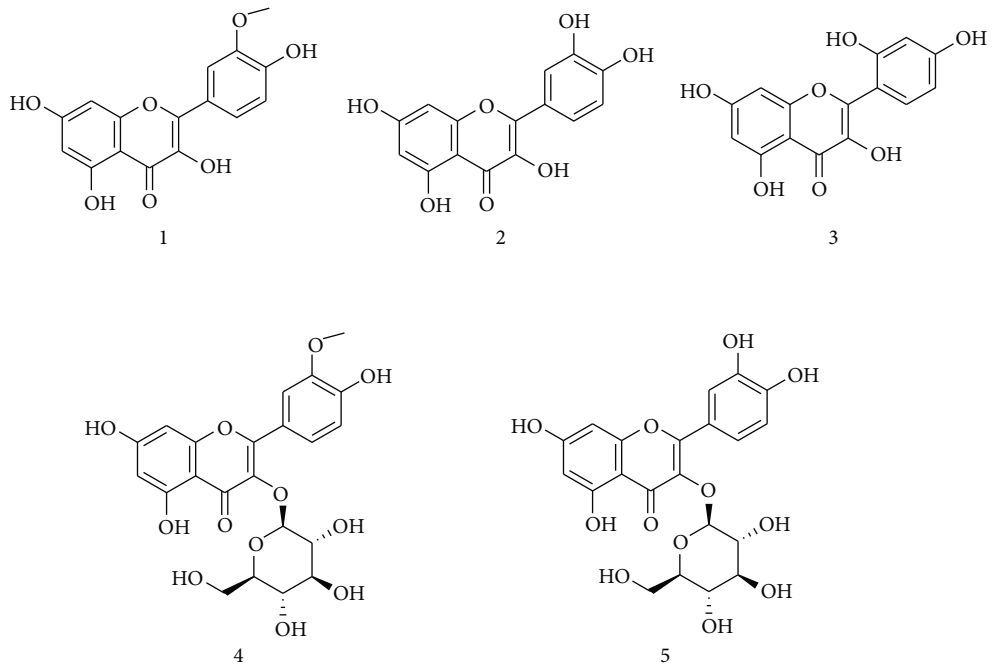

Figure 1: Chemical structure of isolated flavonoid from *A. colchicifolium*.

hydroxy groups at δ_H 9.57, 9.89, 10.95, and 12.58 that corresponded to 3-OH, 4′-OH, 7-OH, and 5-OH, respectively. LC-MS/MS analysis showed molecular ions (*m/z*) at 314 $(M\text{-}H)^-$, 284 (M-H-OCH3), 271 (M-H-OH-CO), and 257 (M-H- OH -CO- CH3), and finally compound **1** was identified as 3′-O-methylquercetin in agreement with isorhamnetin aglycone isolated by Fattorusso and coworkers from *A. ascalonicum* [51].

Compound **2** showed NMR resonances similar to **1** but with no methoxy group in NMR spectra, which is in agreement with quercetin data in the literature [52].

Compound **3** showed a fragmentation pattern similar to flavonoids, including molecular ions (*m/z*) at 301 $(M\text{-}H)^-$, 283 (M-H- OH), 229 (M-H-C2HO2-OH), and 151 (M-H- C8H6O3). The ^{1}H-NMR spectrum displayed two meta doublets at δ_H 6.17 (1H, d, $J = 2.10$) and 6.29 (1H, d, $J = 2.10$) related to H-8 and H-6 at ring A, with an ABX spin system of noncatechol types at δ_H 6.34 (1H, dd, $J = 8.40$, 2.30, H-5′), 6.39 (1H, d, $J = 2.30$, H-3′), and 7.22 (1H, d, $J = 8.40$, H-6′) corresponding to H-5′, H-3′, and H-6′ of B ring, respectively. The ^{13}C-NMR spectra showed 15 signals at δ_C 176.17 (C-4), 163.63 (C-7), 160.88 (C-5), 160.39 (C-2′), 156.76 (C-9, 4′), 148.98 (C-2), 136.20 (C-3), 131.68 (C-6′), 109.15 (C-1′), 106.74 (C-5′), 103.50 (C-10), 102.87 (C-3′), 97.99 (C-6), and 93.32 (C-8) similar to those reported for 2′,3,4′,5,7-pentahydroxyflavone (morin) [53], which was previously reported in other *Allium* species including *A. cepa* peel [54], *A. ampeloprasum* leaves [55], and *A. nigrum* and *A. subhirsutum* bulbs and aerial parts [56].

Compound **4** showed positive reaction to 2-aminoethyl diphenylborinate 1% (flavonoid natural product reagent), with UV spectrum absorption maxima at 251 and 356 nm, characteristic of flavone derivatives. The NMR spectrum of the aglycone moieties showed two *meta*-coupled doublets at δ_H 6.210 (1H, d, $J = 2.14$ Hz) and 6.43 (1H, d, $J = 2.14$ Hz) corresponding to H-6 and H-8, in addition to two *ortho*-coupled proton signals at δ_H 6.91 (1H, d, $J = 8.37$ Hz) and 7.49 (1H, dd, $J = 8.37$, 2.05 Hz) related to H-5′ and H-6′ as well as δ_H 7.95 (1H, d, $J = 2.05$ Hz) related to H-2′. ^{13}C-NMR resonances at 100.78 (C-1″), 77.48 (C-5″), 76.42 (C-3″), 74.36 (C-2″), 69.81 (C-4″), and 60.59 (C-6″) ppm were correspondent to the glucopyranosyl group. Also, δ_c at 98.81, 93.77, and 177.40 ppm was correspondent to (C-6), (C-8), and (C-4), respectively. The glucosyl linkage at C-3 was confirmed by HMBC (Figure 2) correlations between anomeric sugar proton H-1″ as follows: δ_H 5.56 (1H, d, $J = 7.6$) and carbon C-3 (δ_C 132.89), and the configurations were deduced to be β-form based on coupling constants of 7.10 Hz. OCH3 resonance at δ_H 3.83 (3H, s) showed HMBC correlation with C-3′ (δ_C 149.37), and finally **4** was identified as 3′-O-methylquercetin-3-O-β-D-glucopyranoside [57]. It was further confirmed by the negative ESI mass spectrum (Figure 3) at *m/z* 477 $(M\text{-}H)^-$, 447 $(M\text{-}OCH3)^-$, and 315 $(M\text{-}Glucosyl)^-$. The isorhamnetin 3-O- glucoside and other isorhamnetin glycoside derivatives were isolated before from *Allium* spp, including *Allium macrostemon, Allium microdictyon,* and *Allium cepa* [51, 58, 59].

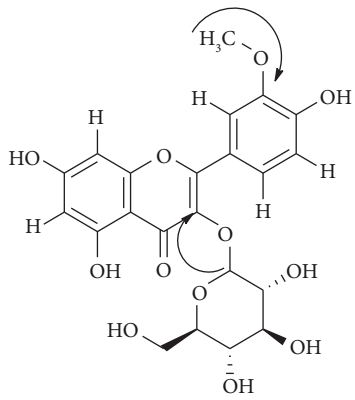

Figure 2: HMBC (H-C) correlated key of compound **4**.

LC-MS/MS analysis of compound **5** revealed a molecular ion at $(M\text{-}H)^-$ 463 m/z. The fragmentation of 463 m/z resulted in the production of (M-H- glucose) 301 m/z, 283 m/z, 270 m/z, and 151 m/z, which is similar to the fragmentation of quercetin glucoside [60]. The ^{1}H-NMR spectra exhibited δ_H: 3.08–3.80 (overlapped, H-2″- H-6″) and the anomeric hydrogen of glucoside moiety at δ_H 5.46 (1H, d, J = 7.10, H-1″) and 5 protons in the aromatic region in accordance with the quercetin aglycone [61]. The ^{13}C-NMR showed similarities to 4 except for lack of methoxy group. Therefore, it was identified as quercetin 3-O-β-D-glucopyranoside in agreement with the literature [62], which is reported in other *Allium* species including *A. Macrostemon* and *A. myrianthum* [58, 63].

Compound **1**: yellow powder, ^{1}H-NMR in DMSO-d6 (400 MHz) ppm δ_H: 3.95 (3H, s 3′-OCH3), 6.31 (1H, d, J = 2.02, H-6), 6.60 (1H, d, J = 2.02, H-8), 7.06 (1H, d, J = 8.41, H-5′), 7.80 (1H, dd, J = 8.41, 2.06, H-6′), 7.87 (1H, d, J = 2.06, H-2′), 9.57 (1H, bs, 3-OH), 9.89 (1H, bs, 4′-OH), 10.95 (1H, bs, 7-OH), 12.58 (1H, bs, 5-OH); ^{13}C-NMR (100 MHz, DMSO-d6) δ_C: 175.83 (C-4),165.87 (C-7), 160.63 (C-5), 156.11 (C-9), 148.78 (C-3′), 147.31 (C-4′), 135.77 (C-3), 121.91 (C-6′), 121.66 (C-1′), 115.47 (C-5′), 111.58 (C-2′), 102.97 (C-10), 98.16 (C-6), 93.56 (C-8), and 55.69 (3′-OCH_3). Negative ESI mass (m/z): $(M\text{-}H)^-$ 314 m/z, 284 m/z, 271 m/z, 257 m/z, and 151 m/z.

Compound **2**: pale yellow powder, ^{1}H-NMR in DMSO-d6 (400 MHz) ppm δ_H: 6.20 (1H, d, J = 1.75 Hz, H-6), 6.43 (1H, d, J = 1.75 Hz, H-8), 6.92 (1H, d, J = 9.92 Hz, H-5′), 7.58 (1H, dd, J = 9.92, 1.7 Hz, H-6′), 7.70 (1H, d, J = 1.7 Hz, H-2′), 12.49 (1H, bs, 5-OH); ^{13}C-NMR (100 MHz, DMSO-d6) δ_C: 175.52 (C-4),164.43 (C-7), 160.63 (C-5), 156.13 (C-9), 147.75 (C-4′), 146.63 (C-2), 145.08 (C-3′), 135.62 (C-3), 121.87 (C-6′), 119.90 (C-5′), 115.60 (C-2′), 114.98 (C-1′), 102.73 (C-10), 98.29 (C-6), and 93.38 (C-8). Negative ESI mass (m/z): $(M\text{-}H)^-$ 301 m/z, 285 m/z, 271 m/z, 255 m/z, 243 m/z, 155, and 151 m/z.

Compound **3**: yellow powder, ^{1}H-NMR in DMSO-d6 (400 MHz) ppm δ_H: 6.17 (1H, d, J = 2.10, H-6), 6.29 (1H, d, J = 2.10, H-8), 6.34 (1H, dd, J = 8.40, 2.30, H-5′), 6.39 (1H, d, J = 2.30, H-3′), 7.22 (1H, d, J = 8.40, H-6′), 12.62 (1H, s, 5-OH), 10.73 (1H, s, 7-OH); ^{13}C-NMR (100 MHz, DMSO-d6) δ_C: ^{13}C-NMR (101 MHz, DMSO-d6) δ 176.17 (C-4), 163.63 (C-7), 160.88 (C-5), 160.39 (C-2′), 156.76 (C-9, 4′), 148.98 (C-2), 136.20 (C-3), 131.68 (C-6′), 109.15 (C-1′), 106.74 (C-5′), 103.50 (C-10), 102.87 (C-3′), 97.99 (C-6), and 93.32 (C-8). Negative ESI mass (m/z): $(M\text{-}H)^-$ 301 m/z, 283 m/z, 229 m/z, and 151 m/z.

Compound **4**: yellow powder, ^{1}H-NMR in DMSO-d6 (400 MHz) ppm δ_H: 3.10–3.80 (overlapped, H-2″- H-6″), 3.83 (3H, s, 3′-OCH3), 5.57 (1H, d, J = 7.10, H-1″), 6.20 (1H, d, J = 2.14, H-6), 6.43 (1H, d, J = 2.14, H-8), 6.91 (1H, d, J = 8.37, H-5′), 7.49 (1H, dd, J = 8.37, 2.05, H-6′), 7.95 (1H, d, J = 2.05, H-2′), 12.62 (1H, s, 5-OH); ^{13}C-NMR (100 MHz, DMSO-d6) δ_C: 177.40 (C-4),164.45 (C-7), 161.24 (C-5), 156.44 (C-2), 156.28 (C-9), 149.42 (C-3′), 146.90 (C-4′), 132.95 (C-3), 122.04 (C-6′), 121.10 (C-1′), 115.23 (C-5′), 113.48 (C-2′), 103.97 (C-10), 100.78 (C-1″), 98.81 (C-6), 93.77 (C-8), 77.48 (C-5″), 76.42 (C-3″), 74.36 (C-2″), 69.81 (C-4″), 60.59 (C-6″), and 55.68(3′ –OCH_3). Negative ESI mass (m/z): $(M\text{-}H)^-$ 477, 314, 299, 284, 271, 257, 243, and 151.

Compound **5**: yellow powder, ^{1} H-NMR in DMSO-d6 (400 MHz) ppm δ_H: 3.08–3.80 (overlapped, H-2″- H-6″), 5.46 (1H, d, J = 7.10, H-1″), 6.19 (1H, d, J = 2.10, H-6), 6.39 (1H, d, J = 2.10, H-8), 6.83 (1H, d, J = 8.86, H-5′), 7.57(1H, dd, J = 8.86, 2.40, H-6′), 7.58 (1H, d, J = 2.40, H-2′), 12.64 (1H, s, 5-OH). ^{13}C-NMR (100 MHz, DMSO-d6) δ_C: 177.39 (C-4),164.22 (C-7), 161.18 (C-5), 156.31 (C-2), 156.15 (C-9), 148.43 (C-4′), 144.78 (C-3′), 121.58 (C-6′), 121.11 (C-1′), 116.12 (C-5′), 115.17 (C-2′), 133.24 (C-3), 103.88 (C-10), 100.78 (C-1″), 98.67 (C-6), 93.52 (C-8), 77.49 (C-5″), 76.42 (C-3″), 74.04 (C-2″), 69.85 (C-4″), and 60.88 (C-6″). Negative ESI mass (m/z): $(M\text{-}H)^-$ 463, 301, 283, 271, and 151.

3.2. Antibacterial, Antibiofilm, and Antiswarming Activities. The result of antibacterial and antibiofilm activities of the crude extract and isolated flavonoids is shown in Table 1. Our results revealed that the crude extract and compounds **3** and **4** showed the highest antibacterial activities against *S. aureus* with MIC_{50} of 25 ± 2.23 μg/ml, 60 ± 3.70 μg/ml, and 73.50 ± 3.20 μg/ml and against *P. mirabilis* with MIC_{50} of 37 ± 3.11 μg/ml, 97.50 ± 6.80 μg/ml, and 133 ± 6.02 μg/ml, respectively. Among the isolated flavonoids, compound **3** showed the most potential against *S. aureus* biofilm formation ($MIBC_{50}$ = 79 ± 5.02 μg/ml) and compound **5** exhibited the most against *P. mirabilis* biofilm formation with ($MIBC_{50}$ = 102 ± 11.01 μg/ml), which was less than the crude extract (Table 1). Besides, our observation showed that compounds (**1–5**) have no considerable effects on the antiswarming activities of *P. mirabilis* although the total extract partially inhibited the swarming of *P. mirabilis* (Figure 4). Flavonoids show antibacterial activities by disrupting bacterial membrane, obstructing bacterial nucleic acid replication, reducing bacterial efflux pump activity, and

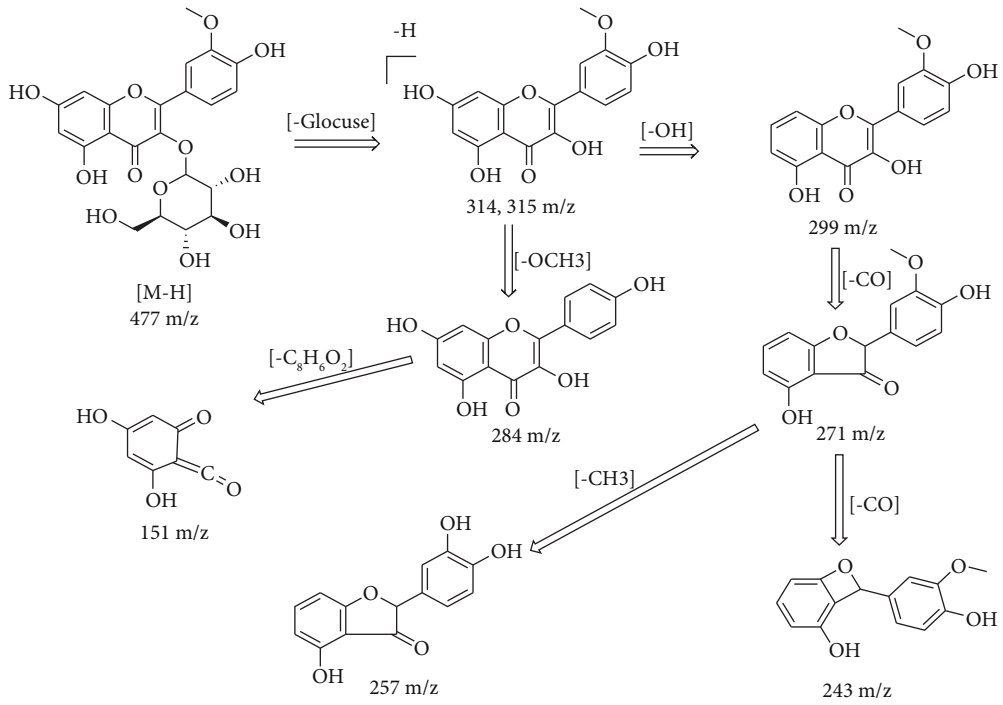

Figure 3: Proposed fragmentation pattern of compound **4** LC-MS/MS spectra analysis.

Table 1: The results of anti-bacterial, anti-biofilm of isolated compounds and crude extract from *A. colchicifolium*.

Compounds	MIC_{50} (μg/ml)		$MIBC_{50}$ (μg/ml)	
	S. aureus	*P. mirabilis*	*S. aureus*	*P. mirabilis*
Compound **1**	481 ± 14.10^{b}	824 ± 8.62^{b}	123 ± 9.01	224 ± 7.80
Compound **2**	100.20 ± 9.20	275 ± 8.70	195 ± 10.31	244 ± 6.20
Compound **3**	60 ± 3.70^{c}	97.50 ± 6.80^{c}	79 ± 5.02^{c}	113.50 ± 7.25
Compound **4**	73.50 ± 3.20^{d}	133 ± 6.02	180 ± 8.02	235 ± 6.21
Compound **5**	206 ± 7.05	385 ± 9.29	239.50 ± 8.23	102 ± 11.01
Crude extract	25 ± 2.23^{a}	37 ± 3.11^{a}	40 ± 2.57^{a}	67 ± 2.01^{a}

[a]: Significant difference of anti-bacterial and anti-biofilm activities between the crud extract and compounds **1**-**5** (Post hoc Tukey, $p < 0.001$). [b]: Significant difference of anti-bacterial activities between the compound **1** and other compounds (Post hoc Tukey, $p < 0.001$). [c]: Significant difference of anti-bacterial and anti-biofilm activities between the compound **3** and other compounds (Post hoc Tukey, $p < 0.001$). [d]: Significant difference of anti- *S. aureus* activities between the compound **4** and other compounds (Post hoc Tukey, $p < 0.01$). After triplicate experiments, all data are shown as mean ± standard deviation (SD).

blocking adenosine triphosphate synthase of bac teria [64, 65]. The presence of hydroxyl groups at positions 5 and 7 and the simultaneous presence of hydroxyl groups in the 2′ and 4′ positions, such as compound **3**, enhance the antibacterial activities of flavonoids. Besides, the presence of glycoside groups attached at position 3, such as compound **4**, increases the effectiveness of flavonoids against bacteria compared to their aglycone form (compound **1**) [66, 67]. Also, compound **5** had the most significant effect on preventing biofilm formation by *P. mirabilis*, which is confirmed by the results of other studies [68].

On the other hand, the formation of biofilm as the production of an extracellular polymer layer by bacteria to adhere to each other and surfaces is a bacterial defence mechanism that increases their resistance to antibacterial agents and causes chronic infections [69]. Flavonoids reveal antibiofilm effects by penetrating biofilm layers and inhibiting bacterial growth and surface adhesion. The presence of a hydrophilic part in the chemical structure of flavonoids, including glycoside and hydroxy groups, such as compound **5**, improves penetration in the biofilm structure and increases antibiofilm activities [64]. However, it seems that compound **3** showed more substantial antibiofilm effects on *S. aureus* by inhibiting growth and killing the bacteria [70]. On the other hand, the higher antibacterial and antibiofilm activities of the crude extract can be related to the presence of other compounds with more potential effects and the synergistic effects of the crude extract compounds [71].

3.3. Antioxidant Activities. All compounds showed prominent antioxidant activities (Table 2 and Figure 5). The DPPH scavenging IC50 of the crude extract and compounds 3 and 2 was $0.60 \pm 0.05\,\mu$g/ml, 0.90 ± 0.03, and $1.02 \pm 0.03\,\mu$g/ml, respectively, more than the ascorbic acid as a positive control (IC50 = $1.21 \pm 0.09\,\mu$g/ml). The DPPH scavenging

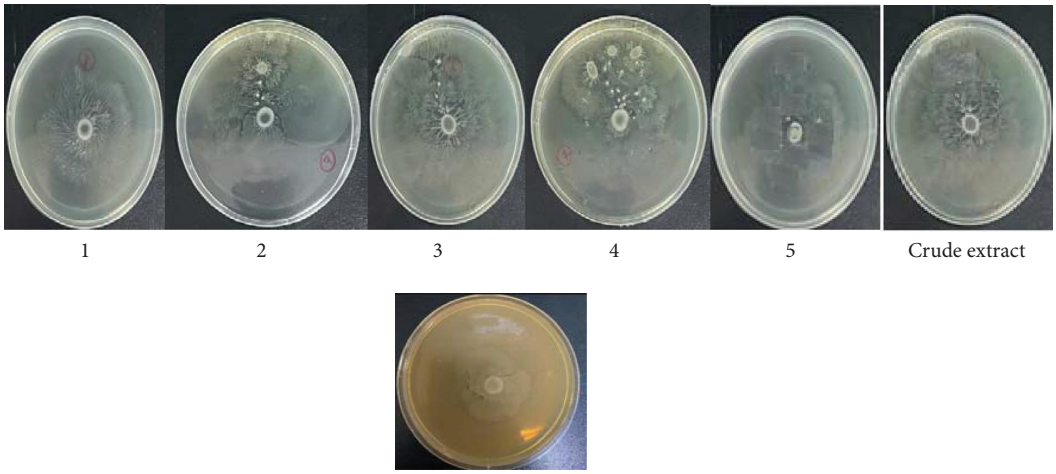

Figure 4: Antiswarming activities of compound **1–5** and the crude extract on *P. mirabilis*.

Table 2: DPPH IC50 (μg/ml) of isolated flavonoid from *A. colchicifolium* leaves.

Compounds	DPPH IC50 (μg/ml)
1	1.40 ± 0.06
2	1.02 ± 0.03
3	0.90 ± 0.03
4	1.61 ± 0.1
5	1.26 ± 0.04
Crude extract	0.60 ± 0.05*
Ascorbic acid	1.21 ± 0.09

* significant difference in DPPH scavenging between crude extract with compounds **1**-**5** and ascorbic acid (Post hoc Tukey, $p < 0.001$). Ascorbic acid was used as a positive control. All experiments were done in triplicate, and data showed mean ± standard division (SD).

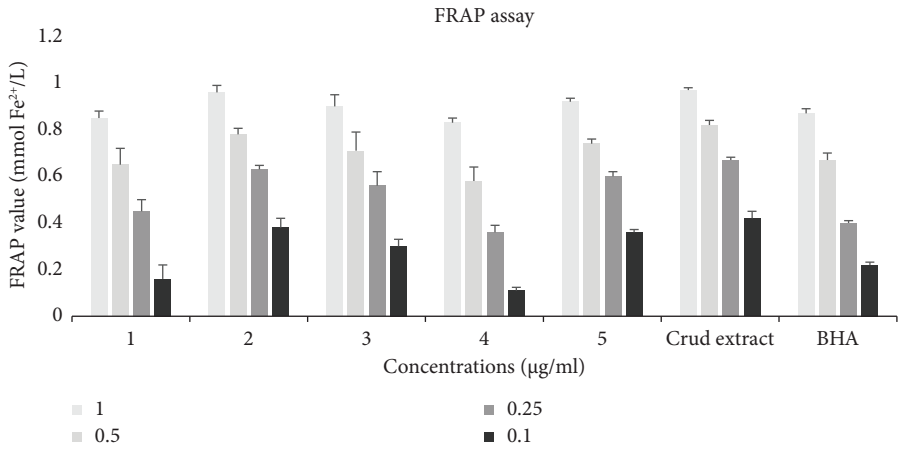

Figure 5: FRAP assay of the isolated compounds (**1–5**) and the crude extract of *A. colchicifolium*. Butylated hydroxyanisole (BHA) was used as a positive control. All experiments were done in triplicate and data were shown as the mean ± standard division (SD).

IC50 (μg/ml) of compounds **4** and **5** was 1.61 ± 0.1 μg/ml and 1.26 ± 0.04 μg/ml, respectively, lower than that of other compounds, crude extract, and ascorbic acid. The higher free radical scavenging potential of compounds **2** and **3** compared to compounds **4** and **5** can be due to the presence of more free hydroxyl groups in their structures [72]. Besides, the crude extract and compound **2** revealed more FRAP values than other compounds and BHA as a positive control in all assayed doses (Figure 5). The FRAP method can show the power of antioxidant compounds in increasing the total antioxidant capacity of serum. The FRAP method principle is based on reducing Fe^{3+} to Fe^{2+} in the presence of antioxidants. Therefore, the reducing power directly relates to the electron-donating properties of antioxidant compounds. The presence of the hydroxyl group in the 5, 2′, and 3′ positions of compound **2** strengthens the resonance power

and enhances electron-donating properties, thereby creating a more stable flavonoid radical of compound **2** against active free radicals [72, 73]. Also, our antioxidant results confirmed with the Nantitanon and Okonogi study. Their study showed that the ability to scavenge free radicals and the reducing power of quercetin is greater than morin, which is related to the more electron-donating properties of quercetin [74].

The synergistic effect of the compounds in the crude extract, as well as the possible presence of strong electron-donating compounds in it, has enhanced the potential power of the antioxidant effect of the crude extract compared to the isolated compounds [26].

3.4. Molecular Docking Results

3.4.1. Molecular Docking of SarA. SarA has a critical role in biofilm formation by *Staphylococcus aureus* [75]. As shown in Table 3, compound **1** with a binding affinity of −7.90 kcal/mol formed 4 hydrogen bonds (Table 3). O2 and O3 in the ether and the hydroxyl groups formed hydrogen bonds with His159 and Tyr142 in chain B, respectively (bond length: 3.01 and 2.70 Å, respectively). O5 and O6 in the hydroxyl groups formed hydrogen bonds with Ser114 and Glu223 in chain A, respectively (bond length: 2.85 and 2.76 Å, respectively). Moreover, Lys121, Leu224, Thr117, and Phe110 in chain A and Glu145 and Asn146 in chain B are involved in these interactions hydrophobically. Compound **2** formed three hydrogen bonds with a binding affinity of −7.8 kcal/mol bound to the SarA. O5 and O6 in hydroxyl groups formed hydrogen bonds with Ser114 and Glu223 in chain A (bond length: 2.92 and 2.75 Å, respectively). Also, a hydrogen bond was found between O1 in the ether group and His159 in chain B (bond length: 3.09 Å). This compound interacted with Lys121, Leu224, Thr117, and Phe110 in chain A and with Tyr142, Glu145, and Asn146 in chain B. Compound **3**, with a binding affinity of −8.10 kcal/mol, formed 4 hydrogen bonds (Table 3, Figure 6(a)). O6 in the hydroxyl group formed two hydrogen bonds with Lys121 and Glu223 (chain A) with bond lengths of 3.12 and 2.81 Å, respectively. Two hydrogen bonds were found between O5 in the hydroxyl group and Ser114 (chain A) (bond length: 2.81 Å) and O1 in the ether group and His159 (chain B) (bond length: 3.13 Å). Thr117, Phe110, and Leu224 in chain A and Glu145, Asn146, and Tyr142 in chain B are involved hydrophobically in the binding. Compound **4** with a binding affinity of −8.1 kcal/mol bound to SarA (Table 3). This compound, through O2 in the ether group and O8 in the hydroxyl group, formed two hydrogen bonds with His 159 (chain B) (bond length: 2.98 and 3.12 Å respectively; Figure 6(b)). Also, O1 in the carbonyl group and O4 in the ether group formed hydrogen bonds with Lys121 (chain A) (bond length: 2.80 and 2.91, respectively). Two other hydrogen bonds were found between O11 and O5 in the hydroxyl groups and Ser114 and Glu223 (chain A) with bond lengths of 3.23 and 3.10 Å, respectively. In addition, this compound hydrophobically interacted with Leu113, Phe110, Leu224, and Thr117 (chain A). Compound **5** has a binding affinity of −7.70 kcal/mol bound to the SarA binding site (Table 3). O1, O4, and O8 in the carbonyl, ether, and hydroxyl groups formed three hydrogen bonds with Lys121 (chain A) (bond length: 2.80, 2.89, and 3.24 Å, respectively). O5 and O11 (in the hydroxyl groups) formed hydrogen bonds with Glu223 and Ser114 (in chain A) with bond lengths of 3.05 and 3.25 Å, respectively. In addition, a hydrogen bond was found between O2 (in the ether group) and His159 (in chain B) (bond length: 3.00 Å). Also, this compound formed several hydrophobic interactions (Leu113, Phe110, Leu224, and Thr117; chain A). The results obtained from the antibiofilm effects of compounds isolated from *A. colchicifolium* on *S. aureus* indicate that compounds **3** and **4** (Table 1) are more effective than other compounds, which are consistent docking study results of these compounds. Therefore, the strong interaction of compounds **3** and **4** with SarA is probably one of the most important mechanisms for preventing the biofilm formation of these compounds. The study conducted by Chemmugil et al. also showed the interaction of morin (compound **3**) with SarA [70].

Table 3: Binding affinity values of the isolated compounds from *A. colchicifolium* with SarA and MrpH.

Ligands	Binding affinity (kcal/mol)	
	SarA	MrpH
Compound **1**	−7.90	−5.50
Compound **2**	−7.80	−5.70
Compound **3**	−8.10	−5.50
Compound **4**	−8.10	−5.80
Compound **5**	−7.70	−6.20

3.4.2. Molecular Docking of MrpH. MrpH, a new member of mannose-resistant/*Proteus*-like (MR/P) fimbriae (MR/P), has a vital role in the biofilm formation by *P. mirabilis* [76]. Compound **1**, with a binding affinity of −5.50 kcal/mol, bound to SarA and hydrophobically interacted with Asn82, Arg118, and Thr116 in the binding site (Table 3). Compound **2** with a binding affinity of −5.70 kcal/mol bound to the binding site of MrpH (Table 3). O5 in the hydroxyl group formed two hydrogen bonds with Thr116 (bond length: 3.16 and 2.87 Å). Also, Asn82, Arg118, and His72 are hydrophobically involved in the binding. Compound **3** with a binding affinity of −5.50 kcal/mol bound to the binding site of MrpH (Table 3). O5 and O7 in the hydroxyl groups formed hydrogen bonds with Asn82 and Thr116 (bond length: 3.16 and 2.96 Å, respectively). This compound hydrophobically interacted with Arg118. Compound **4** with a binding affinity of −5.80 kcal/mol bound to MrpH (Table 3). This compound formed 6 hydrogen bonds, but only one of them was in the binding site (Asn82 with O8 in the hydroxyl group; bond length: 3.14 Å). It interacted with Thr116 and Arg118 hydrophobically. Compound **5**, with higher affinity (−6.20 kcal/mol) compared to others, bound to the binding site of MrpH (Table 3) and formed 4 hydrogen bonds with Asn82 by O6, O8, and O10 in the hydroxyl groups and O4 in the ether group (bond length: 3.24, 3.31, 2.84, and 3.10 Å,

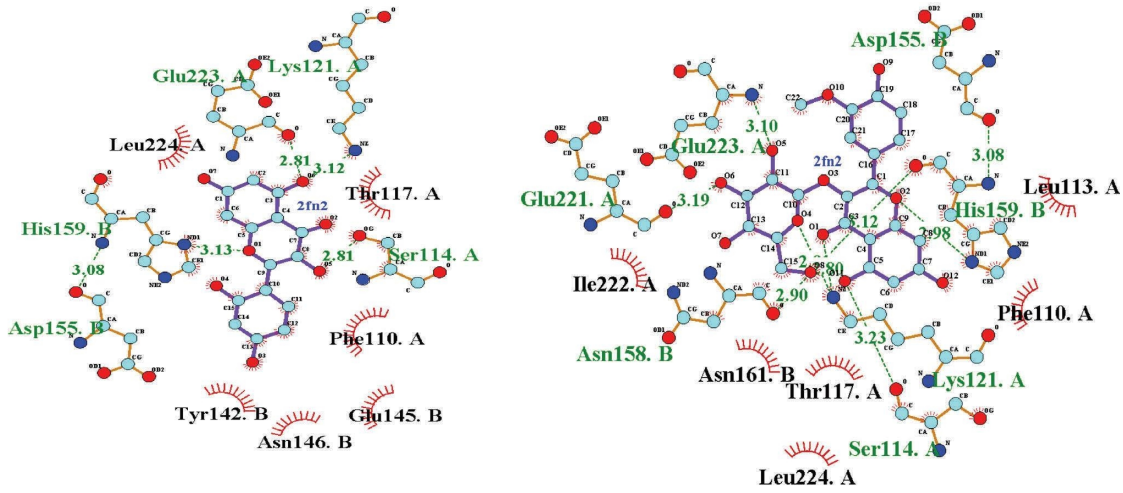

Figure 6: 2D interaction of SarA with (a) compound **3** and (b) compound **4**.

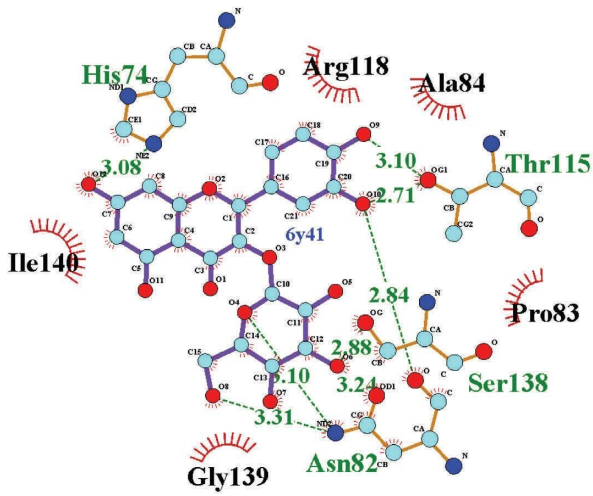

Figure 7: 2D interaction of MrpH with compound **5**.

respectively; Figure 7). Also, a hydrogen bond was found between His74 and O12 (in the hydroxyl group; bond length: 3.08 Å). Moreover, it hydrophobically interacted with Arg118 and Ile140. The results obtained from the studies of the antibiofilm activities of compounds isolated from *A. colchicifolium* on *P. mirabilis* indicated that compound **5** was more effective than other compounds, which is consistent with the results of the strong interaction of this compound with MrpH. So far, no study has been reported on the interaction of the present study compounds with MrpH.

3.5. ADMET Prediction. The results of the compound's ADMET properties are shown in Tables 4 and 5. Compounds **1**, **2**, and **4**, based on Lipinski's rule of 5 (Ro5) [46], are drug likeness, i.e., these compounds have molecular weight (MW) < 500, number of H-bond acceptors (HBA) ≤ 10, number of H-bond donors (HBD) ≤ 5, and MLOGP (lipophilicity) < 4.15. Compounds **4** and **5** with two violations (NorO > 10, NHorOH > 5) are not drug likeness. Also, compounds **1**, **2**, and **3** have topological polar surface area (TPSA) < 140 Å2, which indicates good absorption in the intestine [77]. However, none of these compounds can pass from BBB. Among them, only compound **4** is the P-gp substrate. P-gp mediates the export of a wide variety of chemically diverse compounds out of cells, consequently resulting in limited bioavailability. Also, all of them are noncarcinogens and a weak inhibitor of hERG. The inhibition of hERG channel (cardiac potassium channel) is associated with the prolongation of QT interval and arrhythmia [78]. Taken together, compounds **1**, **2**, and **3** as flavonoid aglycones have better physicochemical and pharmacokinetic properties.

Table 4: Drug-likeness prediction by SwissADME.

Ligands	MW (g/mol)(≤500)	HBA (≤10)	HBD (≤5)	MLOGP	TPSA (Å^2)	Drug likeness
Compound **1**	316.26	7	4	−0.31	120.36	Yes; 0 violation
Compound **2**	302.26	7	5	0.22	111.13	Yes; 0 violation
Compound **3**	302.24	7	5	−0.56	131.36	Yes; 0 violation
Compound **4**	478.40	12	7	−2.37	199.51	No; 2 violations: N or O > 10, NH or OH > 5
Compound **5**	464.38	12	8	−2.59	210.51	No; 2 violations: N or O > 10, NH or OH > 5

MW: molecular weight, HBA: number of H-bond acceptor, HBD: number of H-bond donor, and TPSA: topological polar surface area.

Table 5: Pharmacokinetics and toxicity prediction by SwissADME and admetSAR.

Ligands	BBB permeant	GI absorption	P-gp substrate	Carcinogens	hERG inhibition
Compound **1**	No	High	No	Noncarcinogens	Weak inhibitor
Compound **2**	No	High	No	Noncarcinogens	Weak inhibitor
Compound **3**	No	High	No	Noncarcinogens	Weak inhibitor
Compound **4**	No	Low	Yes	Noncarcinogens	Weak inhibitor
Compound **5**	No	Low	No	Noncarcinogens	Weak inhibitor

BBB: blood-brain barrier, P-gp: P-glycoprotein, GI absorption: gastrointestinal absorption, and hERG: human ether-ago-go-related gene.

4. Conclusion

In addition to the nutritional value, *Allium* plants often have a special place in traditional and complementary medicine in the world. The present study is the first report on the phytochemical investigation and antibacterial, antibiofilm, and antioxidant effects of the *A. colchicifolium* as a native plant in the western regions of Iran from the *Allium* genus. In this study, three flavonoid aglycones, including isorhamnetin (compound **1**), quercetin (compound **2**), and morin (compound **3**), and two glucosylated flavonoids, including isorhamnetin-3-O-glucoside (compound **4**) and quercetin 3-O-glucoside (compound **5**), were isolated and purified from the $CHCl_3$/MeOH (9 : 1) extract of *A. colchicifolium* leaves for the first time. On the other hand, compounds **3** and **5** and the total $CHCl_3$/MeOH (9 : 1) extract had more antibacterial and antibiofilm effects on two pathogenic bacteria, *S. aureus* and *P. mirabilis*. Also, in this study, the interaction of the isolated compounds with two effective proteins in bacterial biofilm formation of SarA and MrpH was investigated. Compounds **3** and **4** showed a strong interaction (−8.1 Kcal/mol) with SarA, and compound **5** showed the highest interaction (−6.2 Kcal/mol) with MrpH. The isolated flavonoids showed low antiswarming activities. Compounds **2** and **3** showed high antioxidant activities in DPPH and FRAP assay. Besides, the ADMET prediction assay showed high GI absorption and safety for compounds **1**, **2**, and **3**. According to the obtained results, the flavonoids in the *A. colchicifolium* leaves can be promising candidates for their use in the pharmaceutical and food industries as antibacterial and antioxidant compounds with natural sources. However, more comprehensive research studies in this regard are suggested for the future.

Data Availability

The data used to support the findings of this study are available from the corresponding author upon reasonable request.

Disclosure

This work was part of the thesis of Mohammad Bagher Majnooni (Pharmacognosy Ph.D. student), Kermanshah University of Medical Sciences, funded with grant number (no. 4000661).

Conflicts of Interest

The authors declare that there are no conflicts of interest.

Acknowledgments

The authors greatly appreciate the Pharmaceutical Sciences Research Center, Isfahan University of Medical Sciences, Iran, for their valuable technical assistance.

References

[1] D. Kothari, W.-D. Lee, K.-M. Niu, and S.-K. Kim, "The genus allium as poultry feed additive: a review," *Animals*, vol. 9, no. 12, p. 1032, 2019.

[2] G. Corea, E. Fattorusso, and V. Lanzotti, "Saponins and flavonoids of Allium t riquetrum," *Journal of Natural Products*, vol. 66, no. 11, pp. 1405–1411, 2003.

[3] J. Sharifi-Rad, D. Mnayer, G. Tabanelli et al., "Plants of the genus Allium as antibacterial agents: from tradition to pharmacy," *Cellular and Molecular Biology*, vol. 62, no. 9, pp. 57–68, 2016.

[4] D. Sobolewska, K. Michalska, I. Podolak, and K. Grabowska, "Steroidal saponins from the genus Allium," *Phytochemistry Reviews*, vol. 15, no. 1, pp. 1–35, 2016.

[5] N. Benkeblia and N. Shiomi, "Fructooligosaccharides of edible alliums: occurrence, chemistry and health benefits," *Current Nutrition & Food Science*, vol. 2, no. 2, pp. 181–191, 2006.

[6] H. Wu, S. Dushenkov, C.-T. Ho, and S. Sang, "Novel acetylated flavonoid glycosides from the leaves of Allium ursinum," *Food Chemistry*, vol. 115, no. 2, pp. 592–595, 2009.

[7] M. Parvu, A. Toiu, L. Vlase, and E. Alina Parvu, "Determination of some polyphenolic compounds from Allium species by HPLC-UV-MS," *Natural Product Research*, vol. 24, no. 14, pp. 1318–1324, 2010.

[8] P. Bonaccorsi, C. Caristi, C. Gargiulli, and U. Leuzzi, "Flavonol glucoside profile of southern Italian red onion (Allium cepa L.)," *Journal of Agricultural and Food Chemistry*, vol. 53, no. 7, pp. 2733–2740, 2005.

[9] D. Kurnia, D. Ajiati, L. Heliawati, and D. Sumiarsa, "Antioxidant properties and structure-antioxidant activity relationship of allium species leaves," *Molecules*, vol. 26, no. 23, p. 7175, 2021.

[10] M. Oh, S.-Y. Kim, S. Park, K.-N. Kim, and S. H. Kim, "Phytochemicals in Chinese chive (allium tuberosum) induce the skeletal muscle cell proliferation via PI3K/Akt/mTOR and smad pathways in C2C12 cells," *International Journal of Molecular Sciences*, vol. 22, no. 5, p. 2296, 2021.

[11] Q. Gao, X.-B. Li, J. Sun et al., "Isolation and identification of new chemical constituents from Chinese chive (Allium tuberosum) and toxicological evaluation of raw and cooked Chinese chive," *Food and Chemical Toxicology*, vol. 112, pp. 400–411, 2018.

[12] Y. Zhou, C. Li, B. Feng, B. Chen, L. Jin, and Y. Shen, "UPLC-ESI-MS/MS based identification and antioxidant, antibacterial, cytotoxic activities of aqueous extracts from storey onion (Allium cepa L. var. proliferum Regel)," *Food Research International*, vol. 130, 108969 pages, 2020.

[13] D. Olennikov, "Flavonol glycosides from leaves of allium microdictyon," *Chemistry of Natural Compounds*, vol. 56, no. 6, pp. 1035–1039, 2020.

[14] D. Kothari, W.-D. Lee, and S.-K. Kim, "Allium flavonols: health benefits, molecular targets, and bioavailability," *Antioxidants*, vol. 9, no. 9, p. 888, 2020.

[15] V. Lanzotti, "Bioactive saponins from allium and aster plants," *Phytochemistry Reviews*, vol. 4, no. 2-3, pp. 95–110, 2005.

[16] Y. Zeng, Y. Li, J. Yang et al., "Therapeutic role of functional components in alliums for preventive chronic disease in human being," *Evidence-Based Complementary and Alternative Medicine*, vol. 2017, Article ID 9402849, 13 pages, 2017.

[17] M. G. Curcic, M. S. Stankovic, I. D. Radojevic et al., "Biological effects, total phenolic content and flavonoid concentrations of fragrant yellow onion (Allium flavum L.)," *Medicinal Chemistry*, vol. 8, no. 1, pp. 46–51, 2012.

[18] K. H. Kyung, "Antimicrobial properties of allium species," *Current Opinion in Biotechnology*, vol. 23, no. 2, pp. 142–147, 2012.

[19] M. A. Farag, S. E. Ali, R. H. Hodaya et al., "Phytochemical profiles and antimicrobial activities of Allium cepa red cv. and A. Sativum subjected to different drying methods: a comparative MS-based metabolomics," *Molecules*, vol. 22, no. 5, p. 761, 2017.

[20] B. X. V. Quecan, J. T. C. Santos, M. L. C. Rivera, N. M. A. Hassimotto, F. A. Almeida, and U. M. Pinto, "Effect of quercetin rich onion extracts on bacterial quorum sensing," *Frontiers in Microbiology*, vol. 10, p. 867, 2019.

[21] F. Nazzaro, F. Fratianni, and R. Coppola, "Quorum sensing and phytochemicals," *International Journal of Molecular Sciences*, vol. 14, no. 6, pp. 12607–12619, 2013.

[22] D. Deryabin, A. Galadzhieva, D. Kosyan, and G. Duskaev, "Plant-derived inhibitors of AHL-mediated quorum sensing in bacteria: modes of action," *International Journal of Molecular Sciences*, vol. 20, no. 22, p. 5588, 2019.

[23] P. Hu, B. Lv, K. Yang, Z. Lu, and J. Ma, "Discovery of myricetin as an inhibitor against Streptococcus mutans and an anti-adhesion approach to biofilm formation," *International Journal of Medical Microbiology*, vol. 311, no. 4, Article ID 151512, 2021.

[24] Y. Fu, W. Wang, Q. Zeng, T. Wang, and W. Qian, "Antibiofilm efficacy of luteolin against single and dual species of Candida albicans and *Enterococcus faecalis*," *Frontiers in Microbiology*, vol. 12, Article ID 715156, 2021.

[25] M. Y. Kim, Y. C. Kim, and S. K. Chung, "Identification and in vitro biological activities of flavonols in garlic leaf and shoot: inhibition of soybean lipoxygenase and hyaluronidase activities and scavenging of free radicals," *Journal of the Science of Food and Agriculture*, vol. 85, no. 4, pp. 633–640, 2005.

[26] I. Demirtas, R. Erenler, M. Elmastas, and A. Goktasoglu, "Studies on the antioxidant potential of flavones of Allium vineale isolated from its water-soluble fraction," *Food Chemistry*, vol. 136, no. 1, pp. 34–40, 2013.

[27] S. Dziri, I. Hassen, S. Fatnassi et al., "Phenolic constituents, antioxidant and antimicrobial activities of rosy garlic (Allium roseum var. odoratissimum)," *Journal of Functional Foods*, vol. 4, no. 2, pp. 423–432, 2012.

[28] R. M. Fritsch and M. Abbasi, "New taxa and other contributions to the taxonomy of Allium L.(Alliaceae) in Iran," *Rostaniha*, vol. 9, no. 2, pp. 1–77, 2009.

[29] M. Abbasi, R. Fritsch, and M. Keusgen, "Wild Allium species used as food and folk medicine in Iran," in *Proceedings of the First Kazbegi Workshop on "Botany, Taxonomy and Phytochemistry of Wild Allium L Species of the Caucasus And Central Asia*, pp. 4–8, Kazbegi, Georgia, June 2007.

[30] S. M. Massoumi, *Introduction to Edible Anthophytes of Kermanshah Province*, Kussar Press, Iran, 2001.

[31] R. Fritsch and M. Abbasi, "A taxonomic review of Allium subg," *Melanocrommyum in Iran*, Gatersleben (IPK), Gatersleben, Germany, 2013.

[32] P. Qin, A. Wei, D. Zhao et al., "Low concentration of sodium bicarbonate improves the bioactive compound levels and antioxidant and α-glucosidase inhibitory activities of tartary buckwheat sprouts," *Food Chemistry*, vol. 224, pp. 124–130, 2017.

[33] A. Harborne, *Phytochemical Methods a Guide to Modern Techniques of Plant Analysis*, Springer Science & Business Media, Berlin, Germany, 2nd edition, 1998.

[34] A. Mirzaei, B. Nasr Esfahani, M. Ghanadian, and S. Moghim, "Alhagi maurorum extract modulates quorum sensing genes and biofilm formation in *Proteus mirabilis*," *Scientific Reports*, vol. 12, no. 1, pp. 13992–14013, 2022.

[35] J. Przekwas, J. Gębalski, J. Kwiecińska-Piróg et al., "The effect of fluoroquinolones and antioxidans on biofilm formation by *Proteus mirabilis* strains," *Annals of Clinical Microbiology and Antimicrobials*, vol. 21, no. 1, pp. 22–10, 2022.

[36] R. Durgadevi, R. Kaleeshwari, T. K. Swetha, R. Alexpandi, S. Karutha Pandian, and A. Veera Ravi, "Attenuation of *Proteus mirabilis* colonization and swarming motility on indwelling urinary catheter by antibiofilm impregnation: an in vitro study," *Colloids and Surfaces B: Biointerfaces*, vol. 194, Article ID 111207, 2020.

[37] M. S. Blois, "Antioxidant determinations by the use of a stable free radical," *Nature*, vol. 181, no. 4617, pp. 1199-1200, 1958.

[38] L. Yin, H. Han, X. Zheng, G. Wang, Y. Li, and W. Wang, "Flavonoids analysis and antioxidant, antimicrobial, and anti-inflammatory activities of crude and purified extracts from Veronicastrum latifolium," *Industrial Crops and Products*, vol. 137, pp. 652–661, 2019.

[39] S. K. Burley, H. M. Berman, G. J. Kleywegt, J. L. Markley, H. Nakamura, and S. Velankar, "Protein Data Bank (PDB): the single global macromolecular structure archive," *Methods in Molecular Biology*, vol. 1607, pp. 627–641, 2017.

[40] R. Thomsen and M. H. Christensen, "MolDock: a new technique for high-accuracy molecular docking," *Journal of Medicinal Chemistry*, vol. 49, no. 11, pp. 3315–3321, 2006.

[41] P. Daisy, S. Mathew, S. Suveena, and N. A. Rayan, "A novel terpenoid from Elephantopus scaber–antibacterial activity on *Staphylococcus aureus*: a substantiate computational approach," *International journal of biomedical science: IJBS*, vol. 4, no. 3, pp. 196–203, 2008.

[42] W. Jiang, W. Ubhayasekera, M. C. Breed et al., "MrpH, a new class of metal-binding adhesin, requires zinc to mediate biofilm formation," *PLoS Pathogens*, vol. 16, no. 8, Article ID e1008707, 2020.

[43] A. C. Wallace, R. A. Laskowski, and J. M. Thornton, "LIGPLOT: a program to generate schematic diagrams of protein-ligand interactions," *Protein Engineering Design and Selection*, vol. 8, no. 2, pp. 127–134, 1995.

[44] M. Nabati and V. Bodaghi-Namileh, "Design of novel drugs (P3TZ, H2P3TZ, M2P3TZ, H4P3TZ and M4P3TZ) based on zonisamide for autism treatment by binding to potassium voltage-gated channel subfamily D member 2 (Kv4. 2)," *International Journal of Networks and Communications*, vol. 6, no. 4, pp. 254–276, 2019.

[45] D. Ranjith and C. Ravikumar, "SwissADME predictions of pharmacokinetics and drug-likeness properties of small molecules present in Ipomoea mauritiana Jacq," *Journal of Pharmacognosy and Phytochemistry*, vol. 8, no. 5, pp. 2063–2073, 2019.

[46] C. A. Lipinski, F. Lombardo, B. W. Dominy, and P. J. Feeney, "Experimental and computational approaches to estimate solubility and permeability in drug discovery and development settings," *Advanced Drug Delivery Reviews*, vol. 23, no. 1-3, pp. 3–25, 1997.

[47] F. Cheng, W. Li, Y. Zhou et al., *admetSAR: A Comprehensive Source and Free Tool for Assessment of Chemical ADMET Properties*, ACS Publications, Washington, DC, USA, 2012.

[48] A. Tesfaye, "Revealing the therapeutic uses of garlic (allium sativum) and its potential for drug discovery," *The Scientific World Journal*, vol. 2021, Article ID 8817288, 7 pages, 2021.

[49] S. Redondo-Blanco, J. Fernandez, S. Lopez-Ibanez, E. M. Miguelez, C. J. Villar, and F. Lombo, "Plant phytochemicals in food preservation: antifungal bioactivity: a review," *Journal of Food Protection*, vol. 83, no. 1, pp. 163–171, 2020.

[50] M. C. Dias, D. C. Pinto, and A. M. Silva, "Plant flavonoids: chemical characteristics and biological activity," *Molecules*, vol. 26, no. 17, p. 5377, 2021.

[51] E. Fattorusso, M. Iorizzi, V. Lanzotti, and O. Taglialatela-Scafati, "Chemical composition of shallot (Allium ascalonicum hort.)," *Journal of Agricultural and Food Chemistry*, vol. 50, no. 20, pp. 5686–5690, 2002.

[52] T. Fossen, A. T. Pedersen, and Ø. M. Andersen, "Flavonoids from red onion (Allium cepa)," *Phytochemistry*, vol. 47, no. 2, pp. 281–285, 1998.

[53] P. K. Agrawal, *Carbon-13 NMR of Flavonoids*, Elsevier, Amsterdam, Netherlands, 1989.

[54] J. Kim, J.-S. Kim, and E. Park, "Cytotoxic and anti-inflammatory effects of onion peel extract on lipopolysaccharide stimulated human colon carcinoma cells," *Food and Chemical Toxicology*, vol. 62, pp. 199–204, 2013.

[55] C. Emir, G. Coban, and A. Emir, "Metabolomics profiling, biological activities, and molecular docking studies of elephant garlic (Allium ampeloprasum L.)," *Process Biochemistry*, vol. 116, pp. 49–59, 2022.

[56] A. Emir, C. Emir, and H. Yıldırım, "Characterization of phenolic profile by LC-ESI-MS/MS and enzyme inhibitory activities of two wild edible garlic: allium nigrum L. and Allium subhirsutum L," *Journal of Food Biochemistry*, vol. 44, no. 4, Article ID e13165, 2020.

[57] D.-M. Wang, W.-J. Pu, Y.-H. Wang, Y.-J. Zhang, and S.-S. Wang, "A new isorhamnetin glycoside and other phenolic compounds from Callianthemum taipaicum," *Molecules*, vol. 17, no. 4, pp. 4595–4603, 2012.

[58] R. Nakane and T. Iwashina, "Flavonol glycosides from the leaves of Allium macrostemon," *Natural Product Communications*, vol. 10, no. 8, Article ID 1934578X1501000, 2015.

[59] D. N. Olennikov, "Flavonol glycosides from leaves of allium microdictyon," *Chemistry of Natural Compounds*, vol. 56, no. 6, pp. 1035–1039, 2020.

[60] R. J. Hughes, T. R. Croley, C. D. Metcalfe, and R. E. March, "A tandem mass spectrometric study of selected characteristic flavonoids," *International Journal of Mass Spectrometry*, vol. 210-211, pp. 371–385, 2001.

[61] S. Panda and A. Kar, "Antidiabetic and antioxidative effects of Annona squamosa leaves are possibly mediated through quercetin-3-O-glucoside," *BioFactors*, vol. 31, no. 3-4, pp. 201–210, 2007.

[62] V. Lanzotti, "The analysis of onion and garlic," *Journal of Chromatography A*, vol. 1112, no. 1-2, pp. 3–22, 2006.

[63] M. O. El Shabrawy, H. A. Hosni, I. A. El Garf, M. M. Marzouk, S. A. Kawashty, and N. Saleh, "Flavonoids from allium myrianthum boiss," *Biochemical Systematics and Ecology*, vol. 56, pp. 125–128, 2014.

[64] A. Biharee, A. Sharma, A. Kumar, and V. Jaitak, "Antimicrobial flavonoids as a potential substitute for overcoming antimicrobial resistance," *Fitoterapia*, vol. 146, Article ID 104720, 2020.

[65] I. Górniak, R. Bartoszewski, and J. Króliczewski, "Comprehensive review of antimicrobial activities of plant flavonoids," *Phytochemistry Reviews*, vol. 18, no. 1, pp. 241–272, 2019.

[66] T. T. Cushnie and A. J. Lamb, "Antimicrobial activity of flavonoids," *International Journal of Antimicrobial Agents*, vol. 26, no. 5, pp. 343–356, 2005.

[67] F. Farhadi, B. Khameneh, M. Iranshahi, and M. Iranshahy, "Antibacterial activity of flavonoids and their structure–activity relationship: an update review," *Phytotherapy Research*, vol. 33, no. 1, pp. 13–40, 2019.

[68] A. Mirzaei, B. Nasr Esfahani, M. Ghanadian, and S. Moghim, "Alhagi maurorum extract modulates quorum sensing genes and biofilm formation in *Proteus mirabilis*," *Scientific Reports*, vol. 12, no. 1, Article ID 13992, 2022.

[69] Z. Khatoon, C. D. McTiernan, E. J. Suuronen, T.-F. Mah, and E. I. Alarcon, "Bacterial biofilm formation on implantable devices and approaches to its treatment and prevention," *Heliyon*, vol. 4, no. 12, Article ID e01067, 2018.

[70] P. Chemmugil, P. Lakshmi, and A. Annamalai, "Exploring Morin as an anti-quorum sensing agent (anti-QSA) against resistant strains of *Staphylococcus aureus*," *Microbial Pathogenesis*, vol. 127, pp. 304–315, 2019.

[71] M. M. N. Perera, S. N. Dighe, P. L. Katavic, and T. A. Collet, "Antibacterial potential of extracts and phytoconstituents isolated from syncarpia hillii leaves in vitro," *Plants*, vol. 11, no. 3, p. 283, 2022.

[72] A. Zeb, "Concept, mechanism, and applications of phenolic antioxidants in foods," *Journal of Food Biochemistry*, vol. 44, no. 9, Article ID e13394, 2020.

[73] P.-G. Pietta, "Flavonoids as antioxidants," *Journal of Natural Products*, vol. 63, no. 7, pp. 1035–1042, 2000.

[74] W. Nantitanon and S. Okonogi, "Comparison of antioxidant activity of compounds isolated from guava leaves and a stability study of the most active compound," *Drug Discoveries & Therapeutics*, vol. 6, no. 1, pp. 38–43, 2012.

[75] J. Morrison, K. Anderson, K. Beenken, M. Smeltzer, and P. Dunman, "The staphylococcal accessory regulator, SarA, is an RNA-binding protein that modulates the mRNA turnover properties of late-exponential and stationary phase *Staphylococcus aureus* cells," *Frontiers in Cellular and Infection Microbiology*, vol. 2, p. 26, 2012.

[76] W. Jiang, W. Ubhayasekera, M. C. Breed et al., "MrpH, a new class of metal-binding adhesin, requires zinc to mediate biofilm formation," *PLoS Pathogens*, vol. 16, no. 8, Article ID e1008707, 2020.

[77] Z. Ya'u Ibrahim, A. Uzairu, G. Shallangwa, and S. Abechi, "Molecular docking studies, drug-likeness and in-silico ADMET prediction of some novel β-Amino alcohol grafted 1, 4, 5-trisubstituted 1, 2, 3-triazoles derivatives as elevators of p53 protein levels," *Scientific African*, vol. 10, Article ID e00570, 2020.

[78] J. T. Milnes, H. J. Witchel, J. L. Leaney, D. J. Leishman, and J. C. Hancox, "Investigating dynamic protocol-dependence of hERG potassium channel inhibition at 37 C: Cisapride versus dofetilide," *Journal of Pharmacological and Toxicological Methods*, vol. 61, no. 2, pp. 178–191, 2010.